MODELLING AND SIMULATION OF FOUR SWITCH THREE PHASE INVERTER FED INDUCTION MOTOR DRIVE USING ANN AT LOW SPEED

[1]T.SIVA KUMAR (M.Tech), [2]I. V.V.VIJETHA (M.Tech), [3]V.S.VAKULA (Ph.D)

[1]Department of Electrical and Electronics Engineering, Vishnu Institute of Technology, Vishnupur village, Bhimavaram, West Godavari District, Andhra Pradesh, INDIA

[2]Asst.Professor, Department of Electrical and Electronics Engineering, Vishnu Institute of Technology, Vishnupur village, Bhimavaram, West Godavari District, Andhra Pradesh, INDIA

[3]Asst.Professor and Head of the Department of Electrical and Electronics Engineering,UCEV ,JNTUK Vizianagaram, Vizianagaram District, Andhra Pradesh, INDIA

[1]sivakumarap2@gmail.com [2]vijetha.i@vishnu.edu.in [3]dr.vakulavs.jntu@gmail.com

ABSTRACT-This paper presents a speed controller utilizing an ANN for indirect field-situated control (IFOC) of acceptance motor (IM) drives nourished by a four-switch three-phase (FSTP) inverter. In the proposed approach, the IM drive system is sustained by a FSTP inverter rather than the conventional six-switch three-phase (SSTP) inverter for savvy low-power applications. The proposed ANN enhances dynamic reactions, and it is likewise outlined with lessened calculation trouble. The total IFOC conspire consolidating the ANN for IM drives encouraged by the proposed FSTP inverter is worked in MATLAB/Simulink. The dynamic execution, robustness, and cold-heartedness of the proposed ANN with the FSTP inverter-bolstered IM drive is analyzed and contrasted with a conventional corresponding necessary (PI) controller under speed tracking, load unsettling influences, and parameters variety, especially at low speeds. It is discovered that the proposed ANN is more robust than the PI and fuzzy controller under load aggravations, and parameters variety. In addition, the proposed FSTP IM drive is equivalent with a customary SSTP IM drive, thinking about its great dynamic execution, cost decrease, and low total harmonic distortion (THD).

INTRODUCTION

VARIABLE-SPEED drives have found widespread use in industrial applications. However, in the household and consumer market their adoption has been sparse. A significant reason that electronic drives have not penetrated the consumer market is their high cost. In a retail marketplace, consumers tend to put little emphasis on "total cost of ownership," including energy costs, and tend to put more emphasis on the initial purchase price and inherent features of the product. In the heating, ventilating, and air-conditioning (HVAC) market, controlling the airflow with an adjustable-speed drive would allow overall system optimization that could significantly reduce energy consumption [1]. Without an adjustable-speed drive, the remainder of the system needs to be oversized, and standby and startup/shutdown losses are significant. In addition to increased efficiency, an adjustable-speed drive used in this application has the potential to hold a tighter temperature band since airflow will always be circulating. It can also be quieter since the system will not be plagued with the starting andstopping noise of both the motor and compressor, as they will operate continuously in a reduced capacity. This paper proposes a new adjustable-speed motor drive system containing a three-phase induction machine and an electronic drive. This paper also proposes a novel current control method for an induction machine that allows for the motor to be speed and/or torque controlled by only three active insulated-gate-bipolar-transistor (IGBT)-type switches. A similar system and control method was proposed in [2], but the system is not physically realizable. This proposed topology with the control method is significant because it has a lower parts count than traditional motor drives. The voltage-source inverter with six switches is standard practice and the use of four switches has also been demonstrated [3]. In addition to the novel topology, the system is focused around a common three-phase induction machine with trivial wiring modifications. As a result, the proposed system achieves full speed control, and maintains good efficiency, at a low comparative cost. The combination of increased performance and lower initial cost will allow for further penetration of adjustable-speed drives into the consumer marketplace.

Usually, the classical control used in motors drive design and implementation has many difficulties, which are as follows. It is on the basis of the mathematical accurate model of the system, that usual it is not known. Drives are nonlinear systems and classical control performance with this system performance decreases. Variation of machine parameters by load variation, motor saturation or thermal variations do not cause expectation performance. With the selected coefficients, classical control cannot receive acceptable results. Voltage source inverter-fed induction motors are most preferred for variable speed drive applications. The controller choice for a SVPWM drive is determined by the requirements of the type of application & is the most successful technique used in meeting the above requirements. Using this type of control, a highly coupled, multivariable nonlinear induction motor can be simply controlled through linear independent decoupled control of the flux and torque, similar to separately excited DC motors. SVPWM method is an advanced, computation intensive PWM method and possibly the best among all the PWM techniques for variable speed drives application. Because of its greater performance characteristics, it has been finding huge number of applications in recent years. With a machine load, the load neutral is normally isolated, which causes interaction among the phases. This type of interaction was not considered before in the PWM discussion. Recently, fuzzy logic control technique has found many applications in the past decades, which overcomes all these drawbacks. Hence, fuzzy logic control technique has the capability to control nonlinear, uncertain systems even in the case where no mathematical model is available for the controlled system. Recently, fuzzy logic control has found many applications in the past decades, which overcomes these drawbacks. Hence, fuzzy logic control technique has the capability to control nonlinearity, uncertain systems even in the case where no mathematical model is available for the controlled system. This project will focus on FLC techniques and the comparison with the classical PI controller.

MOTOR DYNAMICS AND CONTROL SCHEME

A. Mathematical model of IM and Control Scheme

The representation of the IM in a d−q axis was used, and the control structure relies on the IFOC. Detailed explanation of the IFOC model was presented in for non-repetition. The control structure of the proposed FLC-based IFOC of the IM fed by the FSTP voltage-source inverter (VSI) is illustrated in Fig. 1. The speed error between the reference and actual motor speeds and the derivative of speed error are the inputs to the FLC and its output is the reference torque Te∗. The reference currents in d–q axis are transformed into the reference motor currents in a–b–c axis by inverse Park's transformation.

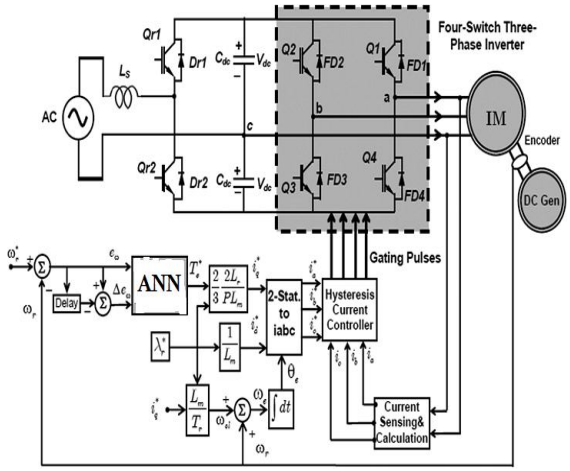

Fig. 1. Block diagram of the proposed FLC-based IFOC scheme of the IM drive fed by FSTP voltage source inverter.

B.FSTP Inverter

Power circuit of an FSTP-VSI-fed IM is illustrated in Fig. 1. This circuit is composed from two sides. The first side is a half-wave voltage doubler fed from a single-phase ac power supply. The frequency of the input ac voltage is fixed; this volt age is rectified using rectifier switches Qr1 and Qr2. The rectifier circuit is utilized to charge the capacitor bank in the dc link. The second side is the FSTP-VSI. The FSTP inverter utilizes four switches: Q1, Q2, Q3, and Q4, respectively, as illustrated in Fig. 1. Phase "a" and phase "b" of the IM are connected through two limbs of the inverter, while phase "c" is connected to the midpoint of the capacitors bank.

TABLE I
FSTP INVERTER MODES OF OPERATION

Switching Function		Switch ON		Output Voltage Vector		
S_a	S_b			V_a	V_b	V_c
0	0	Q_4	Q_3	$-V_{dc}/3$	$-V_{dc}/3$	$2V_{dc}/3$
0	1	Q_4	Q_2	$-V_{dc}$	V_{dc}	0
1	0	Q_1	Q_3	V_{dc}	$-V_{dc}$	0
1	1	Q_1	Q_2	$V_{dc}/3$	$V_{dc}/3$	$-2V_{dc}/3$

Inverter andV_{dc} as follows :

$$V_a = \frac{V_{dc}}{3}(4S_a - 2S_b - 1)$$
$$V_b = \frac{V_{dc}}{3}(-2S_a + S_b - 1)$$
$$V_b = \frac{V_{dc}}{3}(-2S_a - 2S_b + 2) \quad (1)$$

where Vdc is the peak voltage across the storage capacitors; Sa and Sb are the actual states of the two phases "a" and "b" represented by two binary logic variables, which determine the conduction state of the inverter. When Sa is 1, switch (Q1) is conducted and switch (Q4), is not, and when Sa is 0, switch (Q4) is conducted and switch (Q1) is not. Sb has the same principle of operation, and Va, Vb, and Vc are motor phase voltages.

For the balanced generated voltages, the four actual combi nations of the inverter status are lead to four voltage vectors as shown in Fig. 2. Table I illustrates the possible modes of operation and the generated output voltage vector of the FSTP inverter as in.

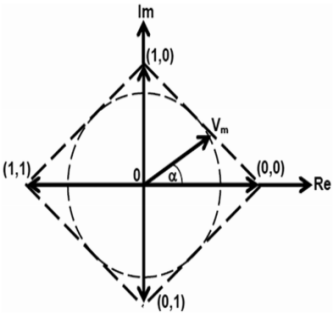

Fig. 2. Switching vectors for an FSTP voltage source inverter

Fig.3(a) outlines the simulation investigation of phase-a current in steady state and its THD at speed 50 r/min under evaluated load conditions utilizing a PI controller with a FSTP inverter-sustained IM drive. To give a reasonable examination, the simulation investigation of steady-state phase-a current and its THD utilizing a FLC with the FSTP-inverter-encouraged IM drive at comparable test conditions are represented in Fig. 3(b). It is observed that the motor phase-a current in steady state and its THD of the proposed FLC with the FSTP-inverter-encouraged IM drive has less THD contrasted and the conventional PI controller. Additionally, the simulation trial of the phase a current in steady state and its THD at speed 50 r/min under appraised load conditions utilizing the FLC with a SSTP inverter-encouraged IM drive is outlined in Fig. 3(c).

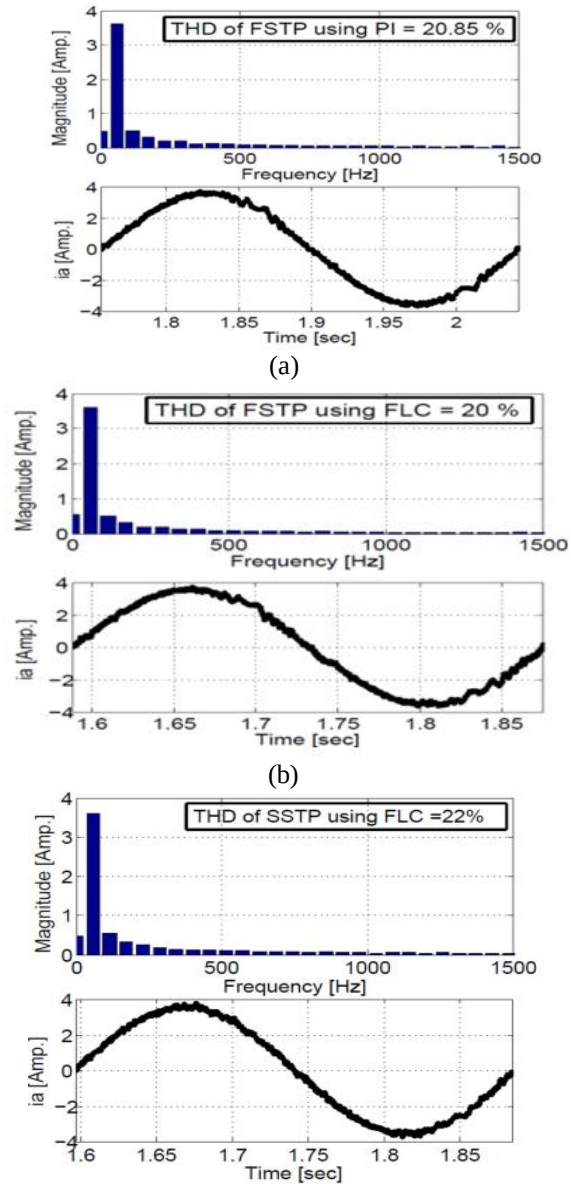

Fig. 3. Simulation results of steady-state phase current ia and its harmonic spectrum at speed 50 r/min under rated load conditions using: (a) PI controller based FSTP inverter-fed IM drive; (b) FLC-based FSTP inverter-fed IM drive; and (c) FLC-based SSTP inverter-fed IM drive.

SPEED CONTROL METHODS

A.FLC Algorithm

The FLC is utilized with an IM to conquer the issue of creating precise mathematical depiction because of load unsettling influences and parameters changing. The contributions to the FLC block are the deviation between the reference and genuine mo

tor speeds (speed blunder) and speed mistake subordinate. These two information sources are used to create the summon torque of an IM (output of the FLC). As delineated in Fig. 1, the reference torque and reference transition are utilized to figure the two reference current components in quadrature and direct pivot (i∗ q, i∗ d), individually.

The FLC has numerous highlights, for example, no requirement for correct mathematical model of an IM, and its activity relying upon linguistic rules with "IF," "AND," and "At that point" administrators. This idea is based on the human logic. The main downside of the FLC is that it needs high count load for simulation and exploratory executions. In this manner, this paper over comes this issue by planning a FLC with low calculation trouble.

Design of Simplified FLC for IM Drive

The dynamic model of IM expressed as follow

$$T_e = \frac{Jdw_r}{dt} + Bw_r + T_L \quad (2)$$

$$T_e - T_L = \frac{Jdw_r}{dt} + Bw_r \quad (3)$$

$$\frac{d\theta_r}{dt} = w_r \quad (4)$$

Where J is the rotor inertia, Te is the electrical torque, TL is the load torque, B is the frication damping coefficient, and ωr is the motor speed.

$$\Delta T_e = \frac{d\Delta w_r}{dt} + B\Delta w_r + \Delta T_L \quad (5)$$

The model of small signal in discrete time for the simplified IM model with applying constant load expressed as

$$\Delta T_e(n) = J\Delta e(n) + B\Delta w_r(n) + \Delta T_L \quad (6)$$

This equation describes the developed electrical torque as a function of motor speed error and change of error as follows:

$$\Delta T_e = \sum_{n=1}^{N} \Delta T_e(n) = f\left(\Delta e(n), \Delta w_r(n)\right) \quad (7)$$

where N is the total number of rules. Δωr(n) = ωr∗(n) − ωr(n) is the speed error; Δe(n) = Δωr(n) − Δωr(n − 1) is the change of speed error; Δωr(n − 1) is the previous sample of speed error; Δωr(n) is the current value of speed error, ωr(n) is the cur rent value of motor speed, and ωr∗(n) is the present sample of reference motor speed.

A MATLAB/Simulink implementation of the FLC is illustrated in Fig. 4. The FLC algorithm of the speed controller employed in the IM drive is based on estimation of two inputs, speed error, and its change as illustrated in Fig. 4

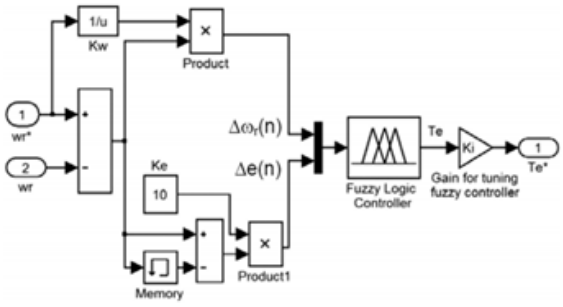

Fig. 4. Block diagram of the FLC using memory block instead of derivative block.

The subordinate block can be supplanted by time-postpone block, which is another approach to get the required info. This time-defer block would permit shortening the computation trouble, in the meantime additionally secure the controller from uncertainties as spikes in the out put, which are the disadvantage of the time-subsidiary block, if the prepared signal change suddenly. The time-postpone block would give a speedier and adequate robust reaction and additionally definitely exact tracking of reference speed. It additionally permits raising the speed sensor inspecting rate essentially.

1.Fuzzification Process:

To plan the proposed FLC, the initial step is to pick the scaling parameters Kw, Ke, and Ki, which are resolved for the fuzzification procedure and accepting the appropriate estimations of the reference torque. The parameters Kw and Ke are resolved so that the standardized estimation of speed mistake and its change, Δωr(n) and Δe(n), individually, remains in satisfactory points of confinement ±1. The parameter for the output signal Ki is resolved so that the evaluated torque is the output of the FLC at all appraised operations.

In this paper, these parameters are thought about constants and are chosen by exploratory experimentation to accomplish the most ideal drive usage. The MF's of Δωr(n), Δe(n), and Te(n) are picked in the wake of choosing scaling parameters. MF's are vital components of the FLC. Fig. 5 demonstrates the MFs utilized for the info and output fuzzy arrangements of the FLC for delivering the reference torque.

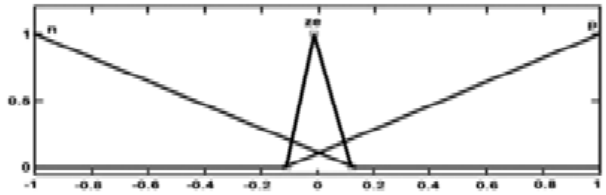

(a)

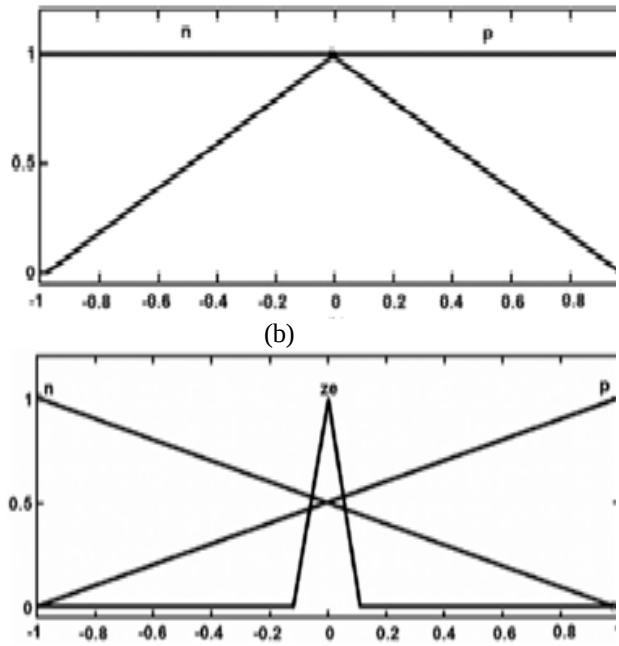

Fig. 5. Membership functions for: (a) speed error Δωr (n); (b) change of speed error Δe(n); and (c) torque reference Te (n) implemented in MATLAB Simulink.

2. Rules Base Process:

The edge of universe of talk of the info vectors Δωr(n) and Δe(n) and output Te(n) are browsed – 1 to 1. The correct fuzzy rule base of the disentangled FLC of the information variables to the output is finished by fuzzy IFAND-THEN logic administrators rules of six semantic articulations as depicted in Table II.

TABLE II
RULES BASE PROCESS

1-	IF $\Delta\omega_r(n)$ is N (Negative) AND $\Delta e(n)$ is N (Negative) THEN $T_e(n)$ is ZE (Zero)
2-	IF $\Delta\omega_r(n)$ is ZE (Zero) AND $\Delta e(n)$ is N (Negative) THEN $T_e(n)$ is P (Positive)
3-	IF $\Delta\omega_r(n)$ is P (Positive) AND $\Delta e(n)$ is N (Negative) THEN $T_e(n)$ is P (Positive)
4-	IF $\Delta\omega_r(n)$ is N (Negative) AND $\Delta e(n)$ is P (Positive) THEN $T_e(n)$ is ZE (Zero)
5-	IF $\Delta\omega_r(n)$ is ZE (Zero) AND $\Delta e(n)$ is P (Positive) THEN $T_e(n)$ is ZE (Zero)
6-	IF $\Delta\omega_r(n)$ is P (Positive) AND $\Delta e(n)$ is P (Positive) THEN $T_e(n)$ is P (Positive)

3.Inference and Defuzzification:

Fuzzy inference is the entire procedure of detailing the mapping of the function from an offered contribution to an output utilizing FL administrators. The Mamdani and Sugeno are the two essential sorts of fuzzy inference techniques.

B.Design of the PI Controller

Choice of the PI controller parameters will impact the speed reaction, its settling time, overshoot esteem, and load torque dismissal, so they ought to be acclimated to have ideal re sponse for a reasonable examination with the proposed FLC.

To outline the PI controller, the schematic diagram of the speed controller of the IM drive is delineated in Fig. 6. The open circle exchange function of (8) has one zero at −Kiω/Kpω , and two shafts at zero and −B/J. The PI controller parameters are intended to have ideal reaction utilizing the root-locus technique for shaft zero areas as cleared up in Fig. 7. The root-locus plot has been utilized to choose the additions of Kiω and Kpω to give the required execution. It is discovered that the PI picks up are Kiω = 15 and K pω = 8 to give the best dynamic reaction.

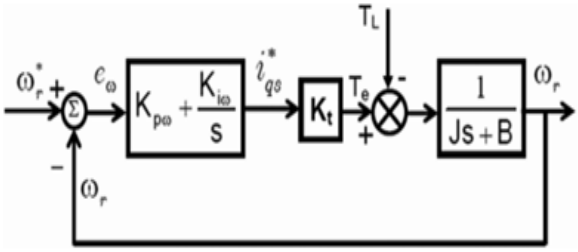

Fig. 6. Block diagram for the speed controller of the IM drive.

$$G_{OL}|_{T_L=0} = \frac{K_{p\omega}K_t\left(s+\frac{K_{i\omega}}{K_{p\omega}}\right)}{(Js+B)s}. \qquad (8)$$

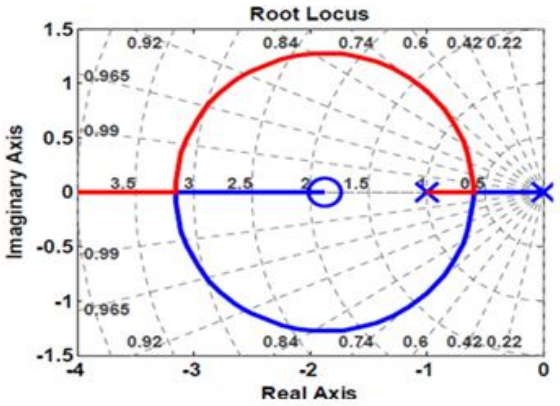

Fig. 7. Root locus plot of the open-loop transfer function with the PI controller gains Kpω = 8 and Kiω = 15

ARTIFICIAL NEURAL NETWORKS (ANN)

The ANNs are difficult to describe with a simple definition. Maybe the closestdescription would be a comparison with a black box having multiple inputs andmultiple outputs which operates

using a large number of mostly parallel connectedsimple arithmetic units. The most important thing to remember about all ANNmethods is that they work bestif they are dealing with non-linear dependencebetween the inputs and outputs.

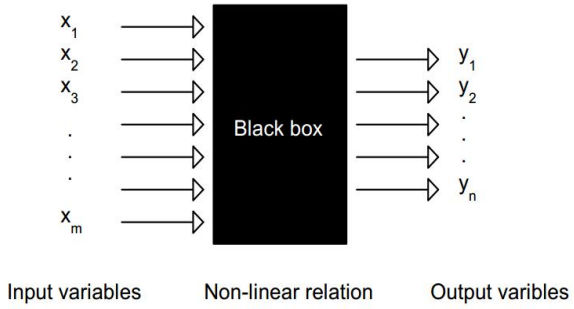

Fig.8 Neural network as a black-box featuring the non-linear relationship

ANNs can be employed to describe or to find linear relationship as well, but thefinal result might often be worse than that if using another simpler standardstatistical techniques. Due to the fact that at the beginning of experiments we oftendo not know whether the responses are related to the inputs in a linear on in a nonlinear way, a good advice is to try always some standard statistical technique forinterpreting the data parallel to the use of ANNs.

Basic concepts of ANNs

Artificial neuronis supposed to mimic the action of a biological neuron, i.e., toaccept many different signals, xi, from many neighboring neurons and to processthem in a pre-defined simple way. Depending on the outcome of this processing,the neuron j decides either to fire an output signal yjor not. The output signal (if it istriggered) can be either 0 or 1, or can have any real value between 0 and 1 (Fig. 11)depending on whether we are dealing with 'binary' or with 'real valued' artificialneurons, respectively.

Mainly from the historical point of view the function which calculates the outputfrom the m-dimensional input vector X, f(X), is regarded as being composed of twoparts. The first part evaluates the so called 'net input', Net, while the second one'transfers' the net input Net in a non-linear manner to the output value y.

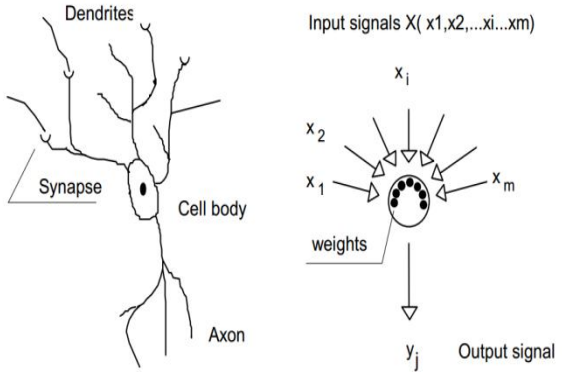

Fig. 9 Comparison between the biological and artificial neuron.

The weights wji in the artificial neurons are the analogues to the real neuralsynapse strengths between the axons firing the signals and the dendrites receiving those signals (Figure 5). Each synapsestrength between an axon and adendrite (and, therefore, each weight) decides what proportion of the incomingsignal is transmitted into the neurons body.

Some possible forms for the transfer function are plotted in Figure 6. It isimportant to understand that the form of the transfer function, once it is chosen, is used for all neurons in the network, regardless of where they are placed or how they are connected with other neurons. What changes during the learning ortraining is notthe function, but the weights and the function parameters that controlthe position of the threshold value, qj, and the slopeof the transfer function aj.(eqs. /2/, /3/).

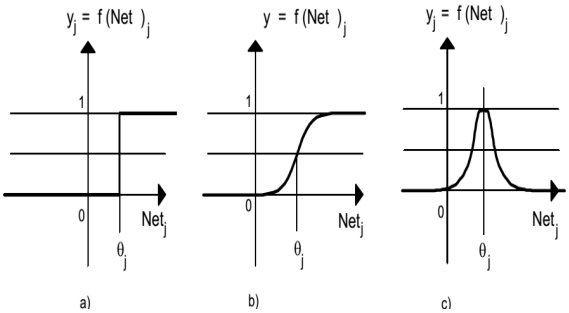

Fig. 10 Three different transfer functions: a threshold (a) a sigmoidal (b) a radial function (c) The parameter qjin all three functions decides the Netjvalue

Artificial neural networks (ANNs)can be composed of different number ofneurons. In chemical applications, the sizes of ANNs, i.e., the number of neurons,are ranging from tens of thousands to only as little as less than ten (1-3). Theneurons in ANNs can be all put into one layer or two, three or even more

layers of neurons can be formed. Figure 8 show us the difference between the one and multilayer ANN structure.

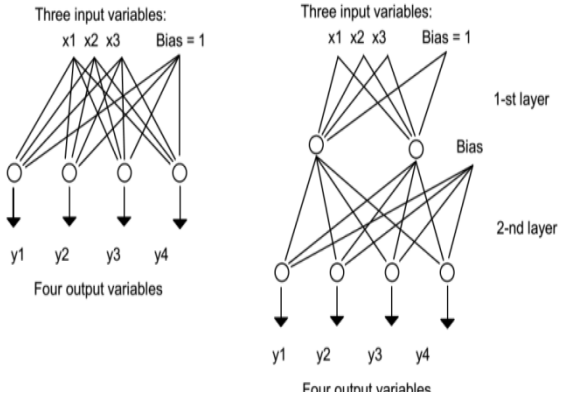

Fig. 11 One-layer (left) and two-layer (right) ANNs.

In Figure 8 the one-layer network has four neurons (sometimes called nodes),each having four weights. Altogether there are 16 weights in this one-layer ANN.Each of four neurons accept all input signals plus the additional input from the biaswhich is always equal to one. The fact, that the input is equal to 1, however, doesnot prevent the weights leading from the bias towards the nodes to be changed!The two-layer ANN (Fig. 8,right) has six neurons (nodes): two in the first layerand four in the second or output layer. Again, all neurons in one layer obtain allsignals that are coming from the layer above. The two-layer network has (4 x 2) + (3x 4) = 20 weights: 8 in the first and 12 in the second layer. It is understood that theinput signals are normalized between 0 and 1.

SIMULATION RESULTS

To approve the viability of the ANN speed controller for the FSTP based-IM drive, a simulation display is worked by MAT LAB/Simulink. The dynamic execution of the proposed IM drive system has been inspected utilizing simulation results under different working conditions.

A.SPEED TRACKING PERFORMANCE

Fig. 12 exhibits reenacted speed and current signals of the FSTP inverter-nourished IM drive utilizing the ANN controller plot, individually, to see the beginning execution. The IM drive begins under light-load torque and a speed charge changed from 0 to 100 r/min. As appeared in Fig. 12, the IM drive utilizing the ANN tracks the coveted speed easily with no overshoot, undershoot, and steady state mistake, while the ANN controller has an overshoot and expansive rising time to arrive the coveted speed as appeared in Fig. 12.

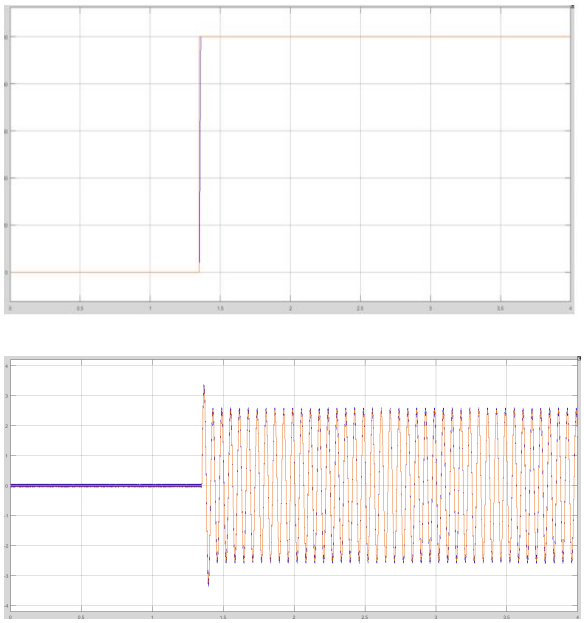

Fig. 12. Simulated speed and stator currents responses of an FSTP inverter fed IM drive for a starting operation at low speed with a step change of a speed reference from 0 to 100 r/min using ANN.

Other recreated speed and stator current reactions at a sudden speed change are delineated in Figs. 13 and 14 for ANN . Additionally, in these cases, the ANN based IM drive guarantees the viability over the customary PI and fuzzy controller as the genuine speed does not has any overshoot, under shoot, and steady-state mistake as appeared in Figs. 13 and 14 when contrasted and the same [see Figs. 13 and 14] utilizing the ANN controller. In this manner, the ANN-based IM drive nourished from the FSTP inverter demonstrates a decent execution under speed reference tracking.

B.LOAD TORQUE DISTURBANCE

For ANN is additionally analyzed for sudden load change at a speed reference 20 r/min as appeared in Fig. 15. At t = 2 s, an appraised torque of 7 N•m is connected. It is discovered that the ANN - based IM drive system affirms the adequacy over the customary PI controller and fuzzy as the real speed has a low speed plunge and recoups rapidly with least time amid sudden load torque, though the stator current quickly lands to the new proportional estimation of the evaluated torque. In this way, great speed tracking execution and great load torque dismissal is accomplished utilizing the ANN-based IM drive, while the PI-Fuzzy controller-based IM drive is unequipped for accomplishing the coveted

execution under the sudden change in the reference speed and torque unsettling influence.

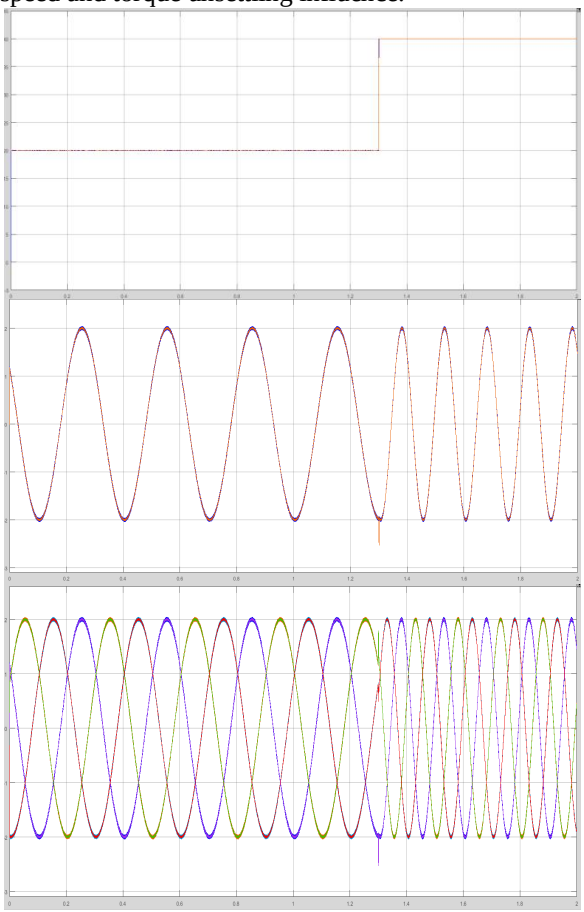

Fig. 13. Simulated speed and stator currents responses of an FSTP inverter-fed IM drive for a step change of a speed reference from 20 to 40 r/min using ANN.

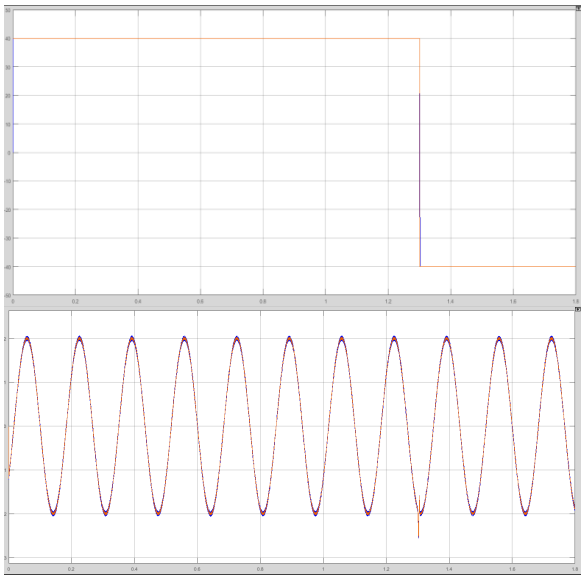

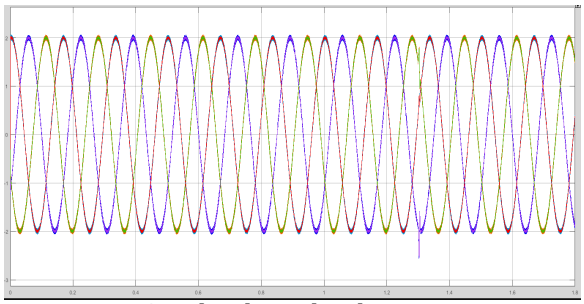

Fig. 14. Simulated speed and stator currents responses of an FSTP inverter-fed IM drive for a speed reversal from 40 to -40 r/min using ANN

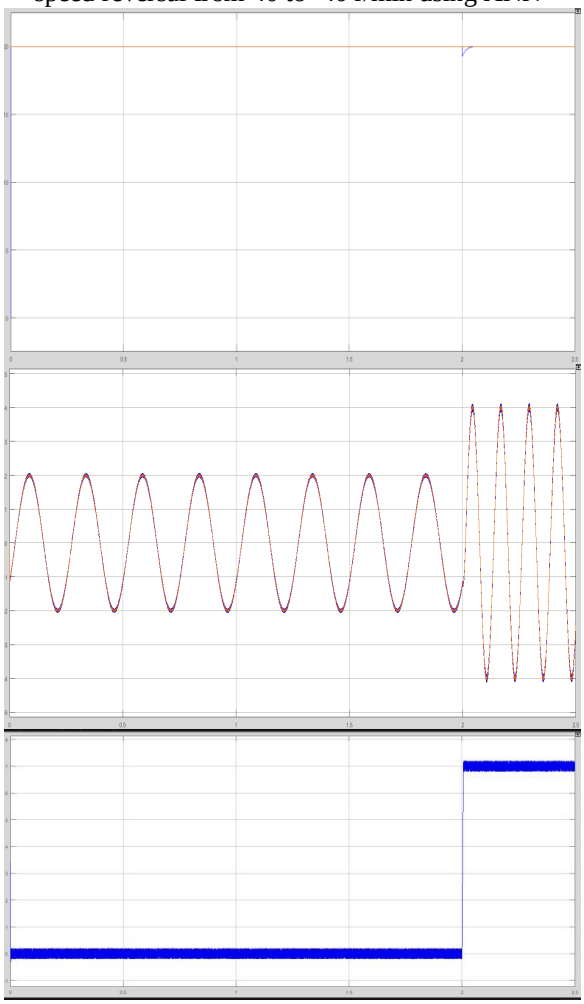

Fig. 15. Simulated speed and stator currents responses of an FSTP inverter fed IM drive for a sudden increase in load of 7 N·m at a speed reference 20 r/min using ANN

C.EFFECT OF PARAMETERS VARIATION

The two speed controllers are analyzed at low speeds under parameters variety. Fig. 16 demonstrates the mimicked reactions of speed, stator currents, and a quadrature current of a FSTP inverter-sustained IM drive for a sudden increment in stator and rotor protections at a speed reference 20 r/min

utilizing the ANN. The confound of 100% in the stator and rotor obstruction esteems is tried to demonstrate the robustness of the ANN. The main chart of Fig. 16 demonstrates the mimicked reference and genuine paces. It is observed that the real speed tracks the reference speed notwithstanding stator and rotor opposition crisscrosses utilizing the proposed ANN. The following diagram demonstrates the stator current.

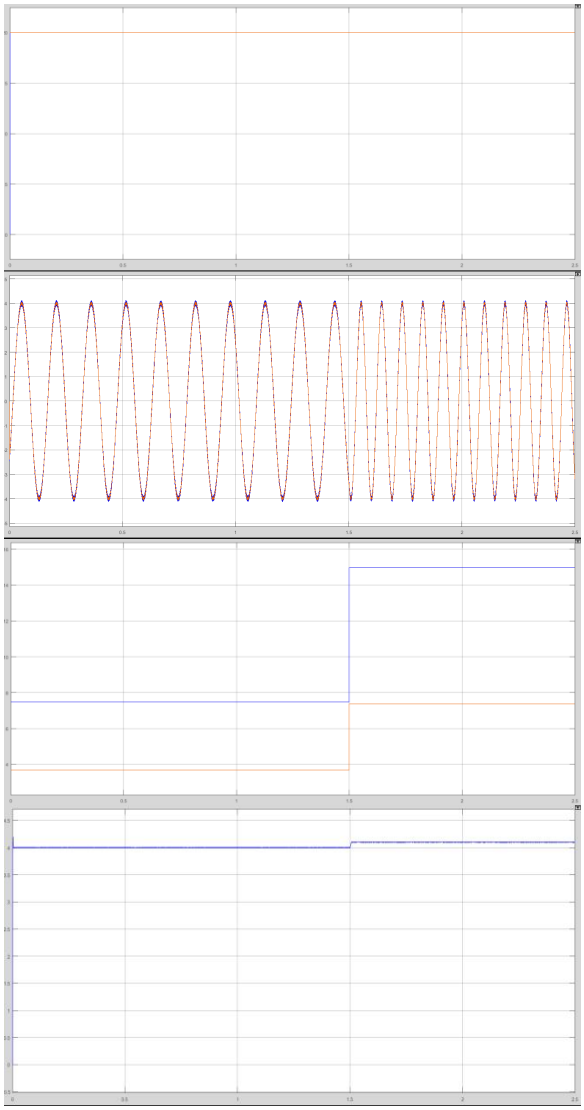

Fig. 16. Simulated speed, stator currents, and quadrature current responses of an FSTP inverter-fed IM drive for a sudden increase in stator and rotor resistances at a speed reference 20 r/min using ANN

Other reproduced reactions under dormancy variety are additionally displayed to inspect the robustness of the two speed controllers. The IM drive is tried with idleness (J = 1.5Jo). Fig. 17 shows recreated speed and direction tracking reactions of a FSTP inverter-sustained IM drive under motor idleness varieties for a speed reference of 20 r/min utilizing the conventional PI controller. A similar figure at indistinguishable conditions is portrayed utilizing the proposed FLC for execution examination purposes as found in Fig.17 legitimizes the robustness of the proposed ANN in contrast with the customary PI and fuzzy controller.

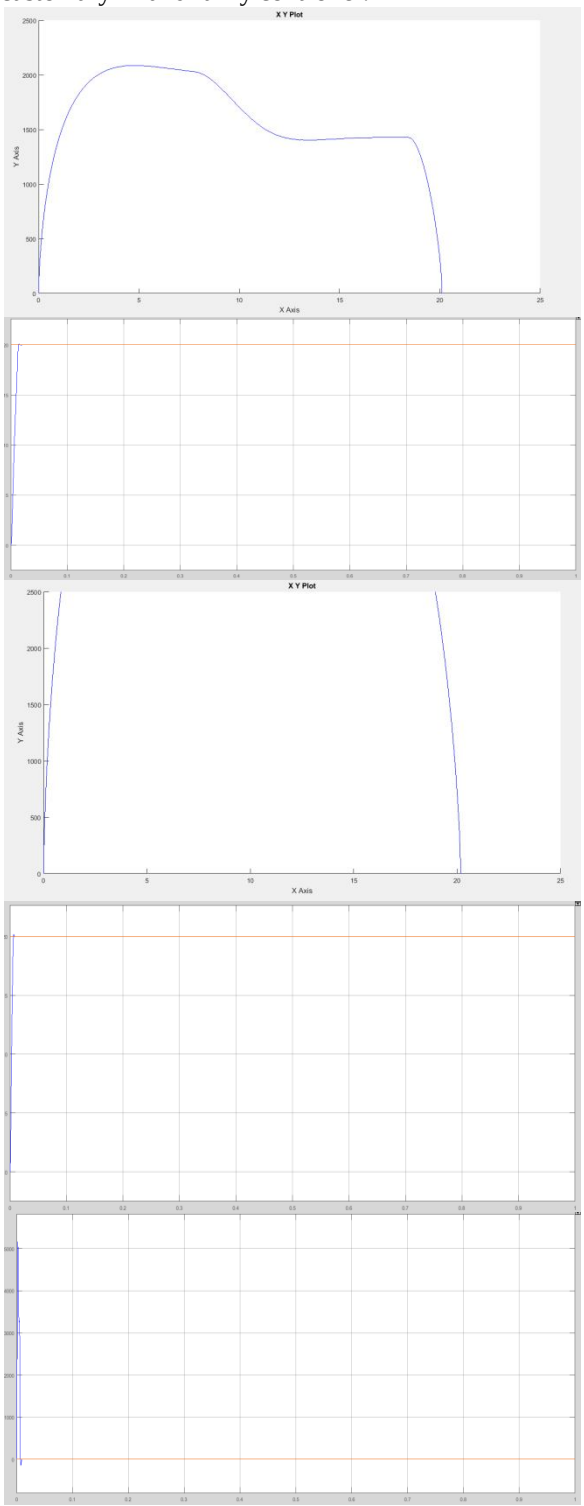

Fig. 17. Simulated speed and trajectory tracking responses of an FSTP inverter-fed IM drive under motor inertia variations for a speed reference of 20 r/min using ANN

CONCLUSION

The proposed ANN-based IFOC for an IM drive sustained by a FSTP inverter has been successfully executed by a PC simulation. The dynamic speed reaction of the IM drive at low speeds is improved utilizing the ANN which is outlined with low calculation weight to be proper for continuous applications. The legitimacy of the proposed ANN has been analyzed both in simulation and experimentation at different speed reference tracking and load torque unsettling influences, especially at low speeds. The robustness of the two controllers has been likewise inspected under parameters variety, particularly motor inactivity, and stator and rotor protections. Similar simulation and trial results show that the proposed ANN of a FSTP inverter-sustained IM drive is better than the PI and fuzzy controller under speed tracking, load unsettling influences, and parameters variety. This demonstrates the great capability of the ANN-based IM drive encouraged by a FSTP inverter for savvy low-power industrial applications.

TABLE IV
PARAMETERS OF IM

Rated power	1.1 kW	Stator leakage inductance	0.0221 H
Rated current	2.545 A	Mutual inductance	0.4114 H
No. of poles	4	Supply frequency	50 Hz
Stator resistance	7.4826 Ω	Supply voltage	380 V
Rotor resistance	3.6840 Ω	Inertia	0.02 kg·m^2
Rotor leakage inductance	0.0221 H	Rated voltage	380 V

REFERENCES

[1] Mohamed S. Zaky,Member,IEEE,and Mohamed K Metwaly, “A Performance Investigation of a Four-Switch Three Phase Inverter – Fed IM Drives at Low Speeds Using Fuzzy Logic and PI Controllers,” IEEE Transactions on Power Electronics, vol. 32, no.5, May. 2017.

[2] H. W. van der Broeck and J. D. van Wyk, “A comparative investigation of three-phase induction machine drive with a component minimized voltage fed inverter under different control options,” IEEE Trans. Ind. Appl., vol. IA-20, no. 2, pp. 309–320, Mar./Apr. 1984.

[3] C. B. Jacobina, M. B. R. Correa, E. R. C. da Silva, and A. M. N. Lima, “Induction motor drive system for low power applications,” IEEE Trans. Ind. Appl., vol. 35, no. 1, pp. 52–61, Jan./Feb. 1999.

[4] C.-T. Lin, C.-W.Hung, and C.-W. Liu, “Position sensorless control for four-switch three-phase brushless DC motor drives,” IEEE Trans. Power Electron., vol. 23, no. 1, pp. 438–444, Jan. 2008.

[5] S. B. Ozturk, W. C. Alexander, and H. A. Toliyat, “Direct torque control of four-switch brushless DC motor with non-sinusoidal back EMF,” IEEE Trans. Power Electron., vol. 25, no. 2, pp. 263–271, Feb. 2010.

[6] C. Xia, Z. Li, and T. Shi, “A control strategy for four-switch three-phase brushless DC motor using single current sensor,” IEEE Trans. Ind. Electron., vol. 56, no. 6, pp. 2058–2066, Jun. 2009.

[7] M. Masmoudi, B. El Badsi, and A. Masmoudi, “DTC of B4-Inverter Fed BLDC motor drives with reduced torque ripple during sector-to sector commutations,” IEEE Trans. Power Electron., vol. 29, no. 9, pp. 4855–4865, Sep. 2014.

[8] K. D. Hoang, Z. Q. Zhu, and M. P. Foster, “Influence and compensation of inverter voltage drop in direct torque-controlled four-switch three-phase PM brushless AC drives,” IEEE Trans. Power Electron., vol. 26, no. 8, pp. 2343–2357, Aug. 2011.

[9] B. El Badsi, B. Bouzidi, and A. Masmoudi, “DTC scheme for a four switch inverter-fed induction motor emulating the six-switch inverter operation,” IEEE Trans. Power Electron., vol. 28, no. 7, pp. 3528–3538, Jul. 2013.

[10] S. Dasgupta, S. N. Mohan, S. K. Sahoo, and S. K. Panda, “Application of four-switch-based three-phase grid-connected inverter to connect renewable energy source to a generalized unbalanced micro grid system,” IEEE Trans. Ind. Electron., vol. 60, no. 3, pp. 1204–1215, Mar. 2013.